Technical Memo

ECMWF
European Centre for Medium-Range Weather Forecasts

889

Investigating biases in the representation of the Pacific sub-tropical jet stream and associated teleconnections (a UGROW sub-project)

F. Vitart, R. Emerton, M. Rodwell, M. Balmaseda, T. Haiden, S. Johnson, L. Magnusson, C. Roberts, I. Sandu

4 January 2022

Series: ECMWF Technical Memoranda

A full list of ECMWF Publications can be found on our web site under:

http://www.ecmwf.int/publications/

Contact: library@ecmwf.int

© Copyright 2022

European Centre for Medium Range Weather Forecasts
Shinfield Park, Reading, Berkshire RG2 9AX, England

Literary and scientific copyrights belong to ECMWF and are reserved in all countries. The content of this document is available for use under a Creative Commons Attribution 4.0 International Public License. See the terms at *https://creativecommons.org/licenses/by/4.0/*.

The information within this publication is given in good faith and considered to be true, but ECMWF accepts no liability for error, omission and for loss or damage arising from its use.

Abstract

UGROW is an ECMWF cross-departmental project focused on Understanding systematic error GROWth from hours to seasons ahead. UGROW-JET, one of the three UGROW sub-projects focuses on biases in the representation of the Pacific sub-tropical jet stream, which plays a key role in the tropical-extratropical teleconnections.

In this study the Pacific sub-tropical jet stream is diagnosed using zonal wind at 300 hPa. An analysis of the model climatology from operational reforecasts reveals that a main issue in the representation of the Pacific sub-tropical jet stream is a westward shift of the eastward extension of the jet stream. This issue can be diagnosed as a negative bias in the 300 hPa zonal wind over the central north Pacific. This bias is the main focus of this study. It is likely to affect the representation of teleconnections originating from the Madden Julian Oscillation (MJO).

The bias increases with lead time up to week 4. It has a strong seasonal variability and is largest in January. It is significantly larger in the control ensemble forecast than in the perturbed ensemble forecasts. This difference is due to the impact of the stochastic physics scheme in the Tropics. A series of sensitivity experiments, where part of the atmospheric circulation is nudged towards ERA5, suggests that there is not a unique source for this bias. However, model errors in the high latitudes seem to be a major contributor. The bias has been considerable reduced in the integrated Forecast System (IFS) cycle 47r3.

1. Introduction

UGROW is an ECMWF cross-departmental project focused on Understanding systematic error GROWth from hours to seasons ahead. It aims to build on and strengthen existing efforts and constitutes an additional channel to bring together scientists from various teams across ECMWF who are interested in identifying ways of enhancing predictive skill, in particular at sub-seasonal timescales (weeks 2-4). In 2021, three UGROW sub-topics were selected: Indian Ocean biases, northern hemisphere summer tropospheric temperature biases and the winter Pacific jet stream bias. This article presents results from the winter jet stream bias sub-topic, which will be referred to as UGROW-JET.

UGROW-JET focusses on biases in the representation of the Pacific sub-tropical jet stream. A main reason for this focus is that the Pacific sub-tropical jet stream is a wave guide for Rossby wave propagation, including those originating from the Madden Julian Oscillation (MJO). Therefore, the Pacific sub-tropical jet stream plays a key role in the representation of MJO teleconnections, a dominant source of predictability at the sub-seasonal time scale. For instance, Lee et al. (2020) showed that the impact of the MJO on Euro-Atlantic weather regimes is much stronger during El-Niño years than during La-Niña years. They suggested that this was due to the impact of ENSO on the Pacific sub-tropical jet stream which retreats to the west during La-Niña years and extends more to the east during El-Niño years. The eastward extension during El-Niño years makes it easier for Rossby waves propagating along the Pacific sub-tropical jet to reach the Atlantic sub-tropical jet and impact the Euro-Atlantic weather regimes. Zhou et al. (2020) also highlighted the importance of the eastward extension of the Pacific jet stream on MJO teleconnections. They found that the eastward shift in the exit region of the subtropical jet caused by the anthropogenic global warming has a stronger impact on MJO teleconnections than the eastward shift of the MJO also caused by the global warming.

One of the main factors limiting the skill of extended-range forecasts over Europe is the representation of MJO teleconnections in the extended-range forecasts of all the models from the World Weather Research Programme (WWRP)/World Climate Research Programme (WCRP) Sub-seasonal to Seasonal prediction (S2S) database (Vitart, 2017). The S2S models represent generally well the pattern of the MJO teleconnections over the northern hemisphere, but the amplitude of the teleconnections is systematically too weak over the Euro-Atlantic region (Vitart, 2017). In particular, the impact of the MJO on the North Atlantic Oscillation (NAO) is significantly weaker in the S2S models, including ECMWF's Integrated Forecasting System (IFS), than in the ERA5 re-analysis. This issue reduces the extended-range predictive skill over Europe. Vitart et al. (2019) discarded the tropical origin of this error: relaxation experiments in which the Tropics (20N-20S) were constrained by the ERA Interim reanalysis showed a very small impact on this particular error. This suggested that the error in the MJO teleconnection lay in the wave propagation rather than the tropical source. Because of the important role of the Pacific sub-tropical jet on MJO teleconnections, biases in the representation of the Pacific sub-tropical jet are likely to have a significant impact on the MJO teleconnections over Europe and therefore are a good candidate to possibly explain the too weak MJO teleconnections over the Euro-Atlantic region. This was the main motivation for UGROW-JET. Another goal of this sub-project was to evaluate the impact of recent model cycles on the jet stream biases.

2. Description of the bias

The Pacific sub-tropical jet bias was diagnosed from the operational reforecasts produced with IFS cycle 46R1 (operational from June 2019 to June 2020). The operational reforecasts cover the previous 20-years, initialized on the same calendar day as the real-time forecasts which are issued on Mondays and Thursdays. Each individual reforecast consists of 11 ensemble members. These are needed to estimate the model climatology. Therefore, the climatology has been computed from a total of 8 start dates per month ×20 years ×11 members=1760 model integrations. In this study, zonal wind at 300 hPa (U300) has been used to diagnose the characteristics of the Pacific sub-tropical jet. Figure 1 shows the 20-year model climatology of U300 computed from this set of re-forecasts and verifying in January for 4 different weekly lead times. According to Figure 1, the jet eastward extension retracts to the west as the lead time increases. The latitudinal position and maximum intensity of the Pacific jet do not vary significantly with lead time. By week 4, the jet stream retreats by about 15 degrees longitude to the west. This bias (relative to the ERA5 reanalysis, Fig.2) is very similar to the impact of a La-Niña event (Fig. 3) which pushes the jet stream westward and, as discussed by Lee et al. (2019), produces weaker teleconnections. Therefore, this bias is likely to be conducive to weaker MJO teleconnections over Europe.

3. Characteristics of the bias

To gain insight into the lead-time dependence of the bias in the representation of the jet, as well as its seasonality and vertical structure, it is convenient to define a bias indicator. We have chosen the spatial average of the zonal wind biases over the area 160E-140W, 30N-40N in the central North Pacific (blue rectangle in Figure 2). Over this area, the bias at week 4 is strongly negative, which corresponds to a westward displacement bias of the Pacific subtropical jet.

An analysis of this bias led to the following conclusions:

- The jet stream extension bias at 300 hPa is seasonal and strongest in January (see Figure 4).
- The bias is strongest at 300 hPa, but still visible at 200 hPa and 500 hPa.
- The wind speed bias (averaged over the box defined in Figure 2) changes with forecast lead time from a positive bias up to day 7 to a strong negative bias in weeks 3 and 4 (see Figure 5).
- The control forecast (i.e. unperturbed member) has a much stronger bias than perturbed forecasts in the extended range (see Figures 5 and 6).
- The bias is modulated by ENSO (stronger in El-Niño years than in La-Niña years).
- At seasonal time scales (3 months into the forecast), the bias is not as strong as at week 4. There is a slight positive impact when increasing resolution from Tco199 to Tco319 and from sub-grid orographic drag changes planned for 48r1. Uncoupled experiments produce a larger jet bias and show a stronger sensitivity to the sub-grid orographic drag changes.
- Biases in the thickness (Z925-Z200) were also analysed and indicate that the control forecast is too cold around 30N. The calculation of the thickness gradient, which corresponds to the thermal wind, between 160E and 160W indicates a weakening of the gradient around 35N in the control forecasts at week 3. This is consistent with the weakening of the jet in that region. This error is larger than in the perturbed forecasts.

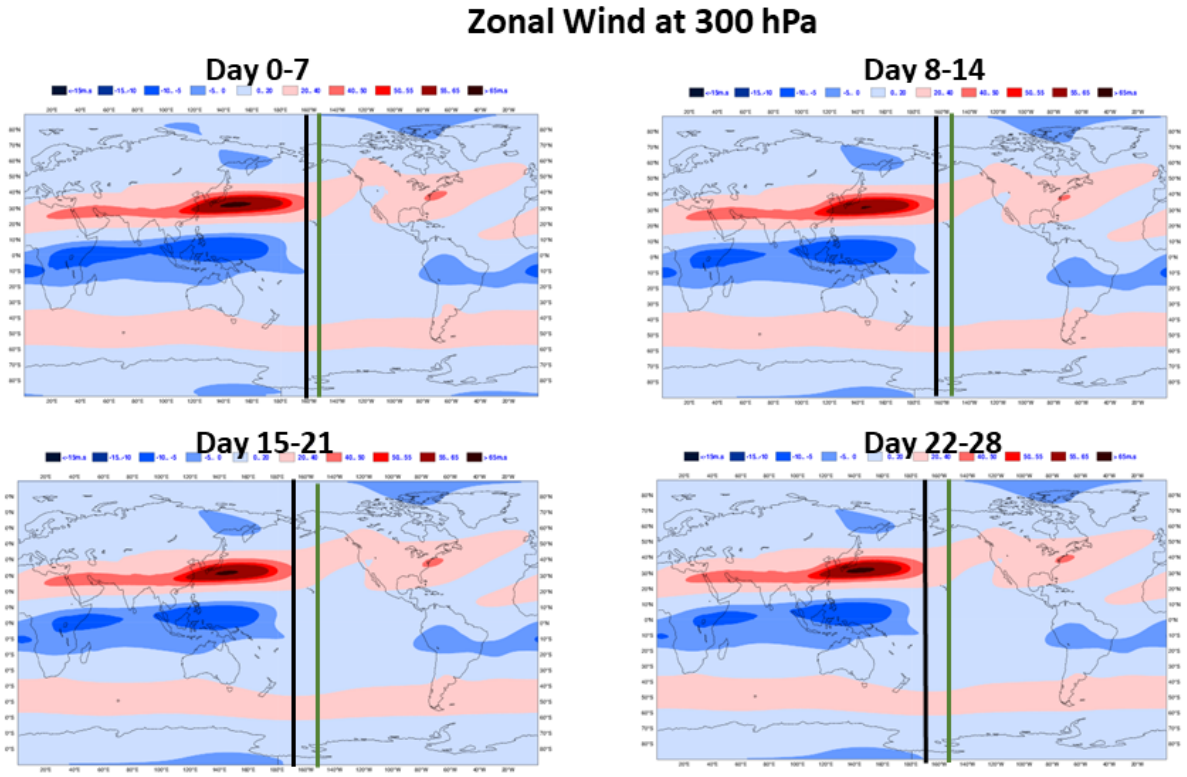

Figure 1: U300 climatology computed from the 46R1 operational 20-year re-forecasts and verifying in January for 4 different lead times; day 0-7 (week 1), 8-14 (week 2), 15-21 (week 3) and 22-28 (week 4). The black vertical line represents the position of the eastward extension of the Pacific sub-tropical jet, identified as the most eastern location with a wind speed larger than 40 m/s. The green vertical line represents this location in the ERA5 reanalysis.

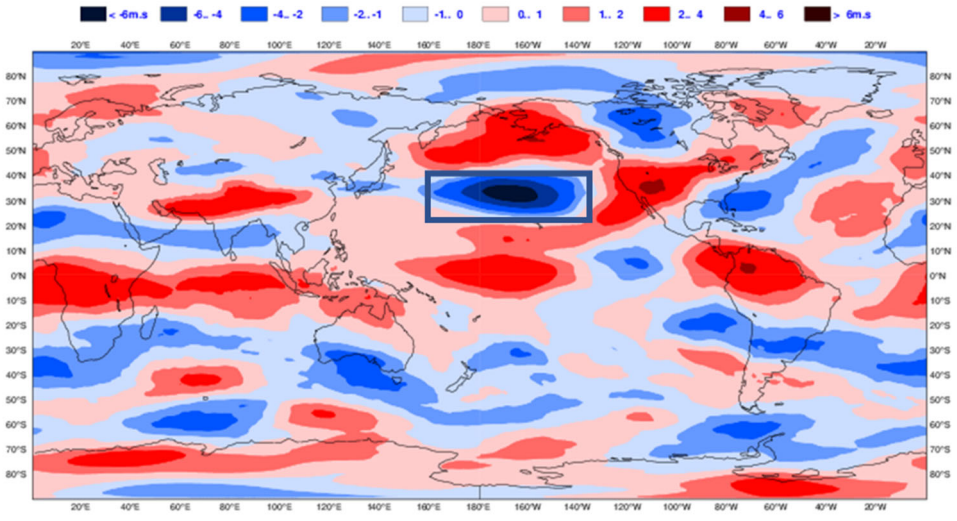

Figure 2: U300 bias in January relative to ERA5 for the period 2000-2018. The forecast lead time is week 4. For some results presented in this article (discussed in section 3), the bias has been averaged over the box 160E-140W, 20N-40N (blue box in the figure)

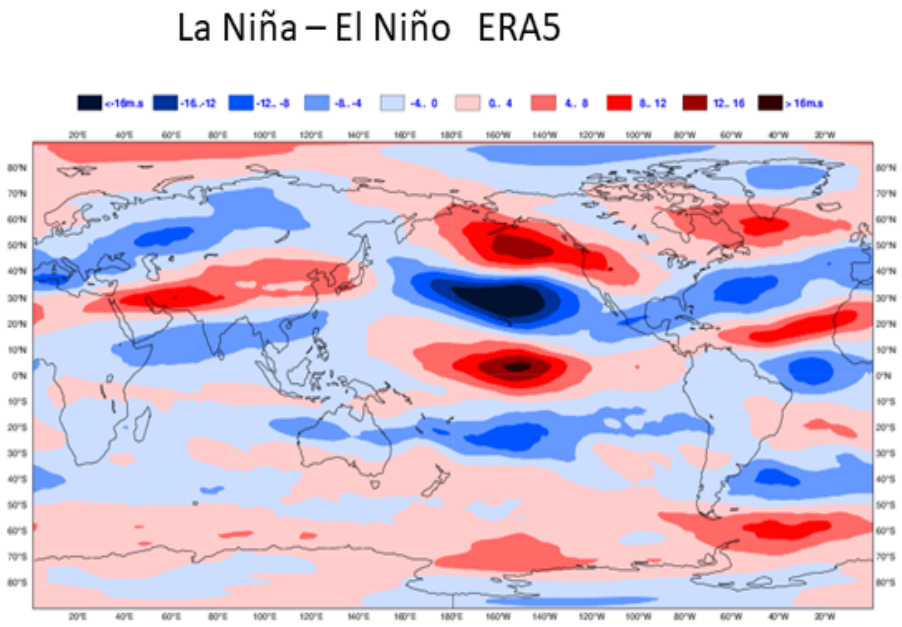

Figure 3: U300 climatology difference between La-Niña and El-Niño years (left panel) in ERA 5

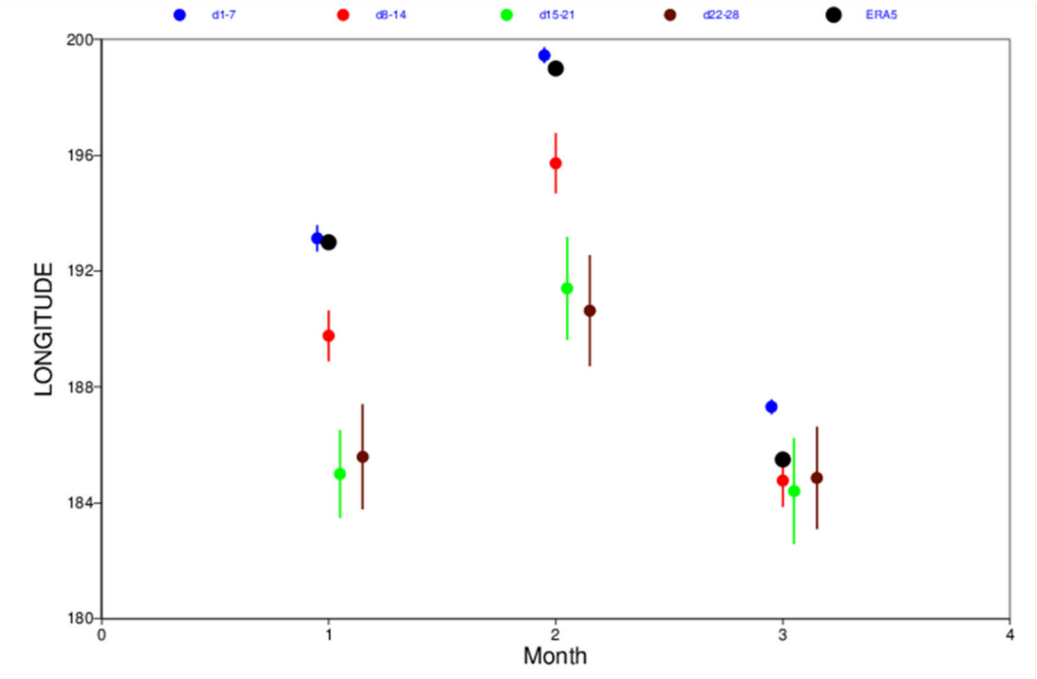

Figure 4: Climatological position of the eastward extension of the Pacific sub-tropical jet in the ECMWF cycle 46r1 operational re-forecasts for different lead times (blue – week 1, red – week 2, green – week 3 and brown – week 4) and verifying months (1 is December, 2 is January and 3 is February). The eastward extension of the jet corresponds to the earliest longitudes of composite mean U300 exceeding 40 m/s. The vertical bars represent 2 standard deviations. ERA 5 is indicated with a

black dot. This figure shows that the bias is larger in December and January and almost disappears in February.

The evolution of the negative jet speed bias with lead time from day 1 to day 10 has been investigated for the winter period 2020-21. At forecast day 1, the bias is centred over the Sea of Japan and then continuously moves eastward, reaching the dateline around day 10. As well as propagating eastward, the negative wind bias over the Sea of Japan amplifies locally with lead time, with most prominent local growth during the winter season. At this location, the wind speed bias may be associated with a cold 500 hPa temperature bias.

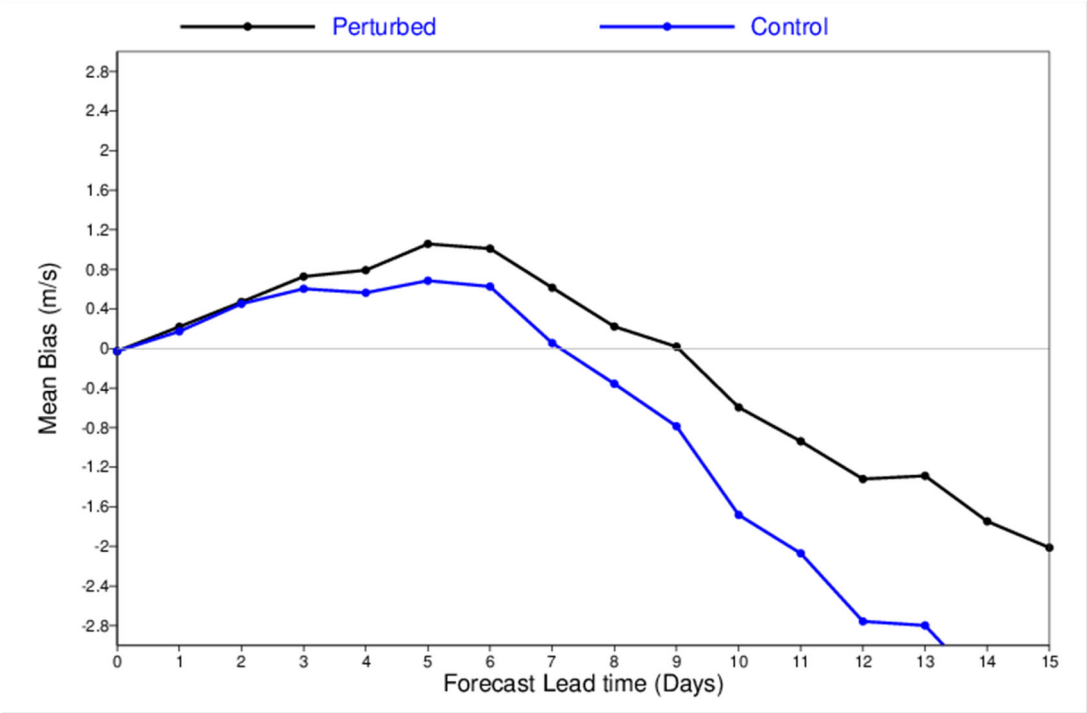

Figure 5: Daily evolution of the U300 bias, averaged over the area 160E-140W, 20N-40N, up to day 15 for the perturbed forecasts (black line) and the control forecast (blue line). This figure shows that the bias changes sign with lead time and that the amplitude of the bias is significantly larger in the control forecasts after 7 days.

The fact that the bias is much stronger in the control forecast than in the perturbed forecasts is likely to be linked to the impact of stochastic physics in the Tropics. This was confirmed by sensitivity experiments where stochastic perturbations (SPPT scheme) where applied only over the northern Extratropics or only over the Tropics. In the experiment where the SSPT scheme was applied only over the northern Extratropics, SPPT had little impact on the Pacific sub-tropical jet stream, unlike in the experiment where SPPT was applied only in the Tropics. Two possible mechanisms could explain this:

- Increased wave activity due to stochastic physics in the Tropics which helps reinforce the sub-tropical jet

- Increased temperature in the Tropics due to stochastic physics which increases the thermal gradient between the North Pole and the Tropics and, consequently, increases the amplitude of the jet stream.

4. Sensitivity to model version

Further investigation has shown that the difference in the bias between the control and perturbed forecasts was reduced with the introduction of cycles 47r2 and 47r3 in May and October 2021. Figure 6 shows that the westward movement of the jet extension with lead time reduced in 47r2 compared to 47r1, although the control forecasts still exhibited a stronger bias than the perturbed forecasts. In 47r3, the westward shift is mostly resolved for the perturbed forecasts and is greatly reduced for the control forecasts, with longer lead times still exhibiting some bias, particularly in week 3. These improvements are likely due to the increased vertical resolution (from 91 to 137 vertical levels) in the operational ensemble forecast integrations introduced in cycle 47r2 and to the changes to the moist physics introduced in cycle 47r3.

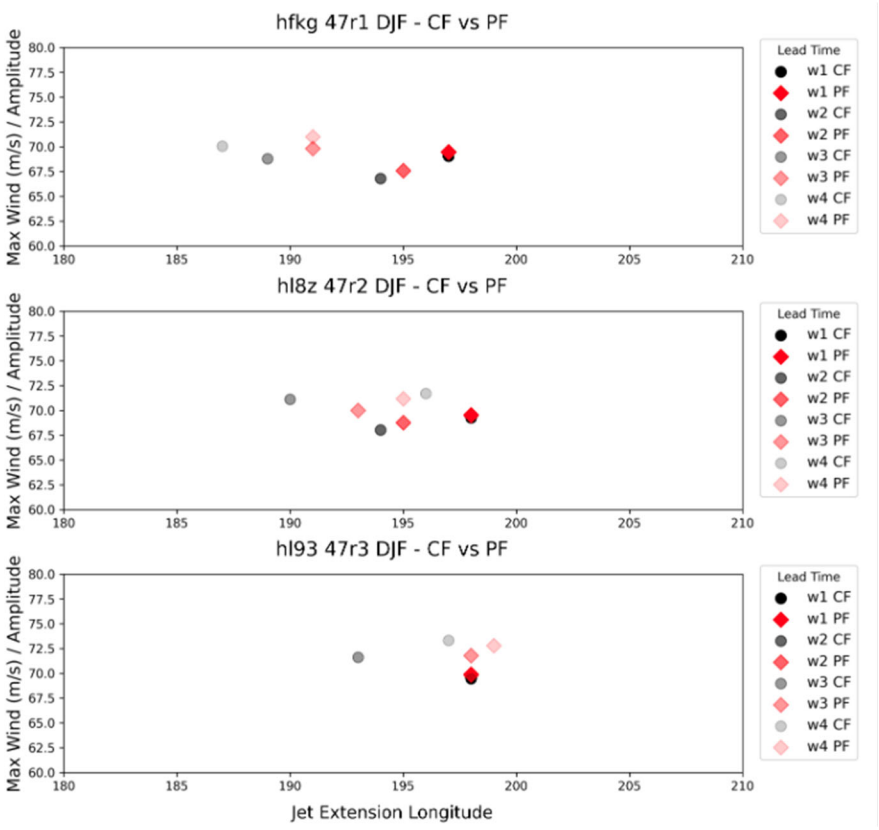

*Figure 6: Scatter plot showing Jet extension (highest longitude of winds exceeding 40m/s) and amplitude (maximum wind) for lead time weeks 1 to 4 (darkest to lightest shading) for the perturbed forecasts (red dots) and control forecasts (grey dots) for IFS cycles 47r1 (top), 47r2 (centre) and 47r3 (bottom). This figure shows the difference in the bias between the control and perturbed forecasts, and the reduction (improvement) with cycle updates. Based on U250 forecasts initialised from the start of each month in DJF from 1989-2016 with 10 ensemble members (3 monthly start dates * 27 years * 10 members = 810 model integrations).*

The bias in U300 has also been diagnosed in several models of the S2S database. Figure 7 suggests that the bias in U300 in the central Pacific, and therefore the bias in the eastward extension of the sub-tropical jet, is a common problem in most of the S2S models. An exception is CFS2 (NCEP model) which displays an opposite bias. Consistent with our hypothesis, this model has the strongest MJO teleconnections over the North Atlantic (Vitart 2017).

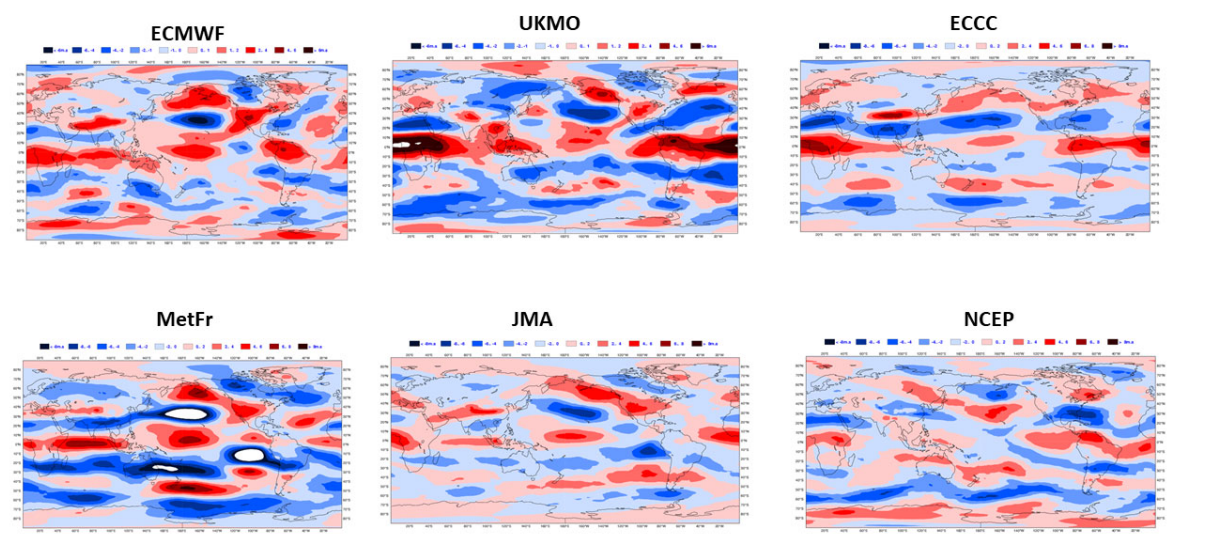

Figure 7: Week 4 U300 bias in January in several models from the WWRP/WCRP S2S database.

5. Impact of the Madden Julian Oscillation (MJO)

In addition to the importance of the position of the Pacific sub-tropical jet for MJO teleconnections for the Euro-Atlantic region, the MJO itself plays a role in modulating the position of the jet (Lee and Lim, 2012). As the MJO propagates eastward through the Tropics, the Pacific sub-tropical jet extends further to the east. The jet is typically at its weakest and shortest when the MJO is active over the Indian Ocean (Phases 2 and 3) and extends further to the east and strengthens when the MJO is active over the Warm Pool and Pacific (Phases 6 to 8). This is shown in Figure 8, which indicates the eastward extension of the jet in each phase of the MJO based on 10-year ERA5 U300 composites.

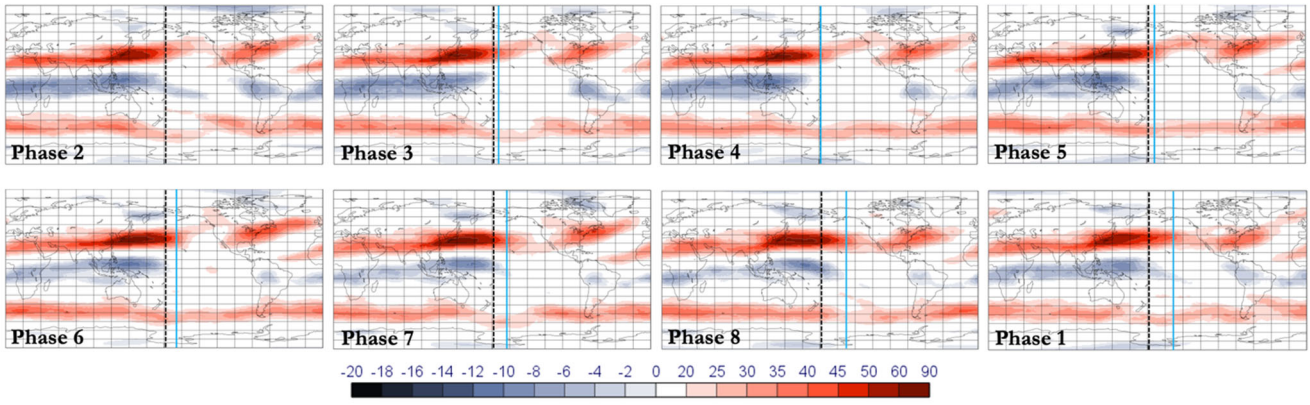

Figure 8: ERA5 U300 composites for days with an active MJO (amplitude ≥ 1) in each phase during the boreal winter season (December-January-February) from 2010 to 2020. The black dashed lines

represent the eastward extension of the jet (most easterly longitude of composite-mean winds exceeding 40m/s) in MJO phase 2, and the blue solid lines represent the eastward extension of the jet in the phase indicated.

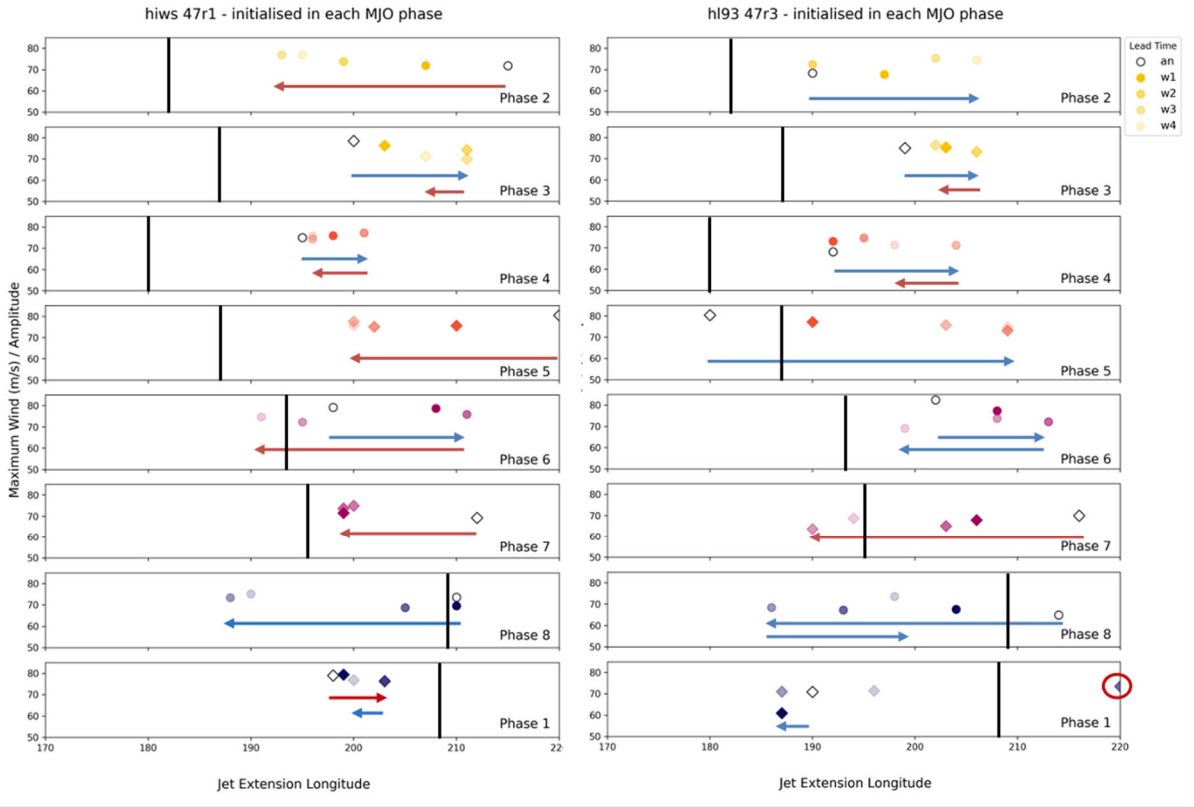

Figure 9: Movement of the Pacific jet extension with lead time in the extended-range forecasts for IFS cycles 47r1 (left) and 47r3 (right), for forecasts initialised in each phase of the MJO. Dots indicate the jet extension longitude and amplitude (maximum wind) for the analysis (forecast day 0, black open markers) and forecast weeks 1 (darkest shading) to 4 (lightest shading), and the arrows indicate the direction of movement with lead time. Blue arrows indicate that the forecasts display the expected movement of the jet extension with progression of the MJO, and red arrows indicate that the forecasts do not capture the expected movement of the jet. Two arrows indicate a change in direction during the forecast horizon. The vertical black lines indicate the ERA5 climatological position of the jet extension for each MJO phase (equivalent to the blue lines in Figure 8).

As part of UGROW-JET, the ability of the IFS to capture this observed modulation of the jet by the MJO was investigated. The diagnostics shown in Figure 9 indicate the movement of the jet extension with lead time for forecasts initialised in each phase of the MJO. For forecasts initialised in phases 2 and 3, some eastward movement would be expected at longer lead times, and for forecasts initialised in phases 4 and 5, eastward movement would be expected at all lead times. Forecasts initialised in phases 6 and 7 should see some eastward movement at short lead times followed by a westward shift, and phases 8 and 1 may see a westward shift followed by another eastward shift, if the MJO remains active and returns to phase 2 over the Indian Ocean. In 47r1, this modulation of the jet extension by the MJO was generally not captured; the longitude at which the forecasts are initialised does not correspond well with climatology (progressing further to the east moving down the plots, as demonstrated in Figure 8

by comparing the position at forecast day 0 (open black markers) with the ERA5 climatological position for each phase (black vertical lines)), with the westward shift bias noticeable for most phases. In 47r3 however, the modulation of the jet by the MJO is significantly improved, with most phases showing movement of the jet in the expected direction. This improvement is likely due to the change in moist physics introduced in cycle 47r3. An exception is phase 7, and phases 3 and 4 at longer lead times. In general, the initial position is better captured in 47r3, with the jet extension furthest west in phases 2 to 4, moving east through phases 5 to 1. While the longitude at which the forecasts are initialised would not be expected to correspond exactly with climatology, there remains an issue with the initial position particularly in phases 7 and 1, despite the overall improvement in this modulation of the position with the MJO. It is noted that sample sizes for the conditional evaluation by MJO phase in 47r3 are small, ranging from 18 to 81 ensemble members (2 - 9 start dates) depending on the phase.

The U300 wind biases relative to ERA5 were also calculated for two subsets of the 20-year extended-range operational reforecasts performed with 46r1, initialised with an active MJO in each phase, and initialised in some MJO phases exhibiting a larger bias. Forecasts initialised while the MJO is active over the Indian Ocean (phases 2 and 3) were found to have the largest bias at lead times when the MJO would be moving across the Maritime Continent and into the West Pacific (weeks 3 and 4), when the jet typically extends further to the east. An example is shown in the left panel of Figure 10, for week 3 biases relative to ERA5 when forecasts are initialised in phase 3. As such, the impact of the so-called Maritime Continent Barrier Effect - whereby the MJO is often significantly weakened when propagating eastward into the Maritime Continent region - was investigated, particularly given the typically poor simulation of the barrier effect in NWP models (Jiang et al., 2020). Ensemble members initialised with an active MJO in phase 3 were grouped according to whether the forecast RMM timeseries progressed through MJO phases 4 and 5, reaching phase 6 for at least 1 day. Overall, 37.6% of ensemble members correctly predicted the MJO to cross the Maritime Continent (of the members that predicted the MJO would cross, 78% were correct, but of the members that predicted the MJO would not cross, 55% were incorrect and the real-world event did cross the Maritime Continent). The jet biases were still present in the forecasts that correctly propagated the MJO across the Maritime Continent, and the jet position and strength were similar in ensemble members that crossed compared to those that did not cross (regardless of whether the real-world event crossed), suggesting that the error in crossing the Maritime Continent Barrier Effect is not a driver of the jet bias.

The jet bias was however reduced in 47r3 in those phases that exhibited larger biases relative to ERA5 in 46r1 (based on 47r3 experiments (hl93) initialised from the start of each month in DJF, for 1989-2016 with 10 ensemble members). Figure 10 provides a comparison of the jet biases relative to ERA5 in 46r1 and 47r3, for week 3 forecasts initialised in MJO phase 3. Such a comparison is more challenging for some phases for which the sample size of ensemble members is much smaller, but overall 47r3 shows a reduction in the westward bias particularly for forecasts initialised in phases 2 and 3, but in some phases appears to introduce an eastward bias. Forecasts that were predicting an active MJO in a given phase at a given lead time were also evaluated (not shown), and while 46r1 generally placed the jet extension too far west with increasing lead time for all phases, 47r3 shows a marked improvement at capturing the furthest east extension of the jet in phases 8 and 1.

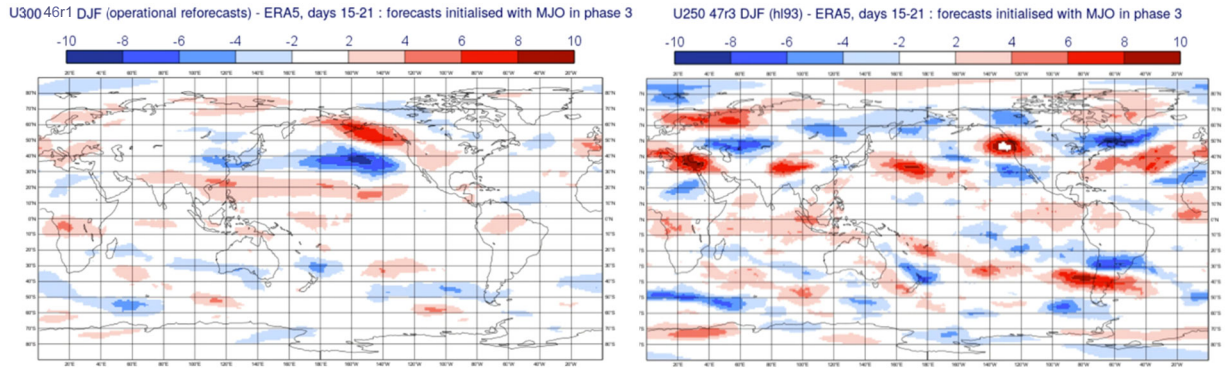

Figure 10: U300 (46r1, left) and U250 (47r3, right) week 3 biases relative to ERA5, for forecasts initialised with an active MJO in phase 3 during DJF, based on 500 ensemble members for 46r1 and 81 ensemble members for 47r3.

6. Sensitivity experiments

In order to identify the sources of the jet bias, a series of relaxation experiments has been run, in which the IFS is nudged towards ERA5 over specified domains. In addition, sensitivity experiments have been performed to test the impact of the turbulent orographic drag and turbulence parametrizations on the Pacific sub-tropical jet bias. All these experiments were produced using the same configuration:

- 46-day integrations
- 11-member ensemble
- Atmospheric resolution: Tco319 with 137 vertical levels
- 1-degree ocean model with 75 vertical levels
- Start dates: 12/16/19/23/26/30 December 1999-2018 and 2/6/9 January 2000-2019

6.1 Tropical relaxation experiment

In this experiment, the tropical band (10N-10S) has been nudged towards ERA5 and an 11-member ensemble has been run with cycle 47R1 for 32 days starting on the same dates as the operational 20-years re-forecasts produced with 46r1 (in the winter 2019-2020). The nudging uses a 12-hour forcing timescale. Figure 11 shows the U300 biases in the reference experiment (same setup but without nudging) and the tropical nudging experiment. According to Figure 11, the bias in the central North Pacific associated with the Pacific subtropical jet is significantly reduced when nudging the Tropics. This indicates that a significant portion of the bias originates from errors in the Tropics, but errors in the Tropics cannot explain the entire bias. In this tropical relaxation experiment, the control and perturbed forecast display a very similar bias in U300 and Pacific jet eastward extension. This confirms that the difference between control and perturbed forecasts in Figure 5 comes from the Tropics and most likely from the impact of stochastic physics on the tropical climate.

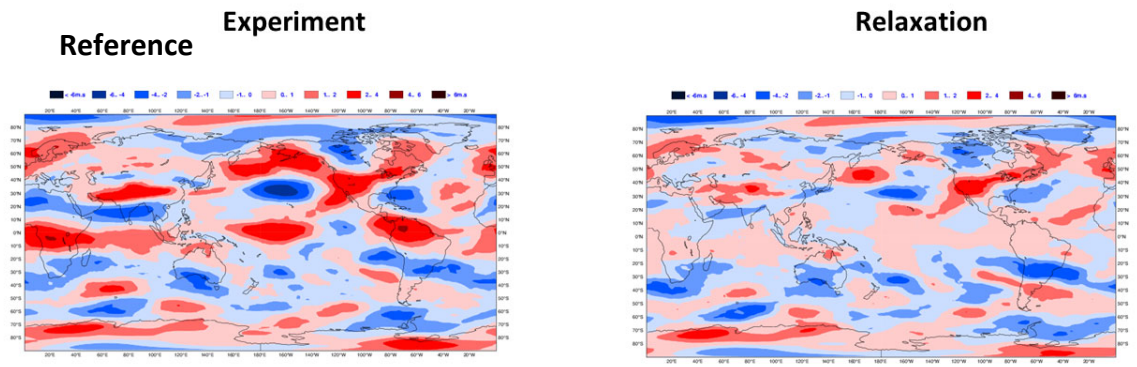

Figure 11: U300 biases at week 4 in the reference experiment (left) and tropical relaxation experiment (right).

This relaxation experiment provides an opportunity to diagnose the evolution of model errors originating from the tropics. Systematic day-2 errors in the control reforecast experiments for DJF 2000-2016 show anomalous upper-level convergence over the 'Warm Pool' region (also known as the 'Maritime Continent', around Indonesia) as seen in the divergent wind errors (vectors) in Figure 12(a). (There are also large errors over South America, but these are not a focus of this investigation). The convergence error over the Warm Pool would be consistent with too little convective heating. Associated with this error is a strong and statistically significant mean 'equatorial Rossby-wave' response (streamfunction dipole error straddling the equator; contours), which extends well into the sub-tropics. Shading shows the mean error in the 'Rossby Wave Source': the forcing of vorticity by the divergent wind. In the context of this study, notice in particular the mean Rossby Wave Source error at the head of the Pacific Jet around 160^{o}E (near Japan) with magnitude ~$3\times10^{-11}s^{-2}$. Figure 12(b) shows the day-2 impact of relaxing towards ERA5 within the band 10^{o}S to 10^{o}N (note the change in shading interval from $2\times10^{-11}s^{-2}$ to $8\times10^{-11}s^{-2}$). The relaxation corrects mean errors in the relaxation band (by construction) and also well into the subtropics – including the Rossby wave dipole centred on the Warm Pool region and the Rossby wave forcing near Japan.

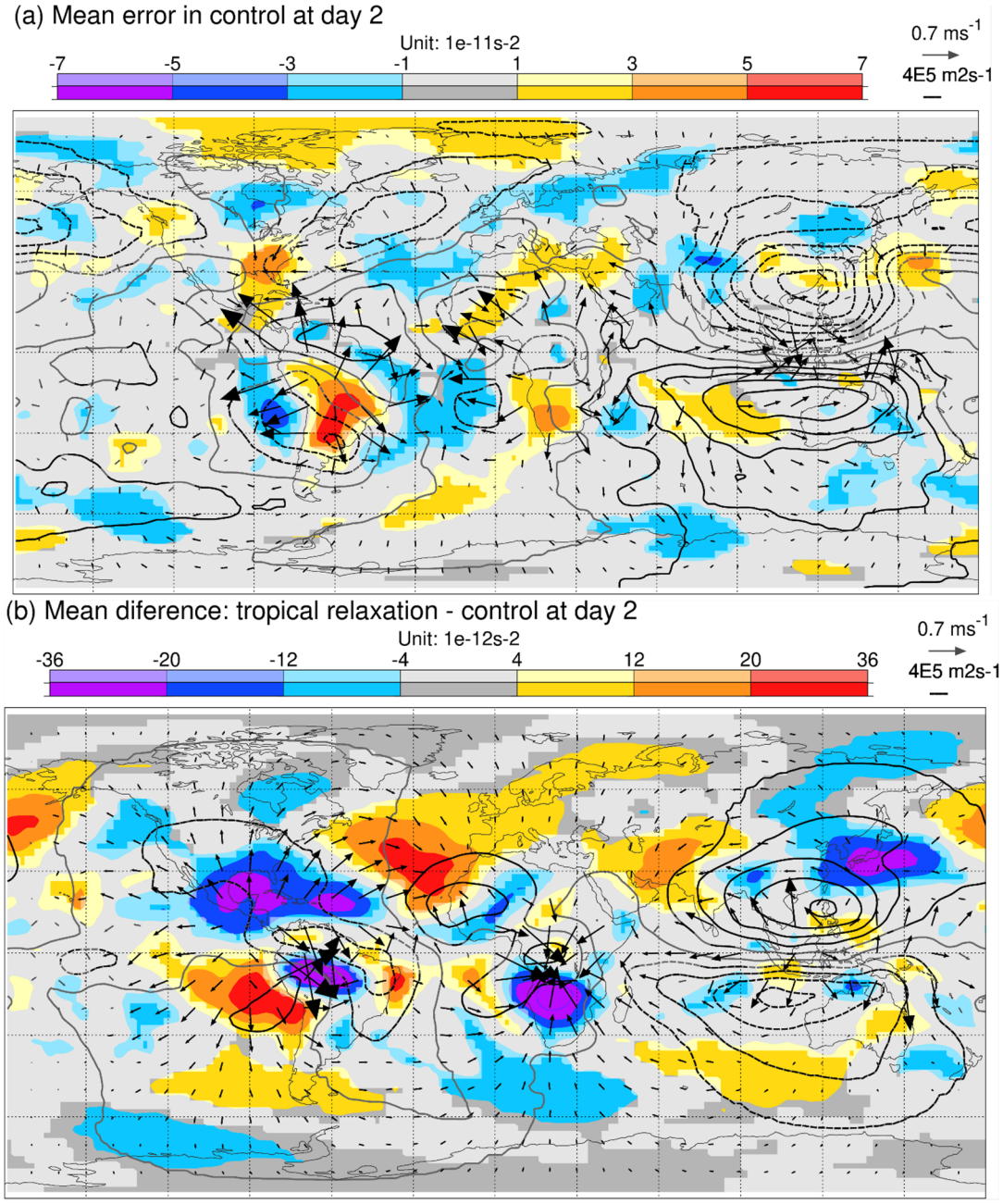

Figure 12 Plots based on the control (unperturbed) reforecasts covering the period DJF 2000-2016 and equivalent reforecast experiments where the circulation (vorticity, divergence and temperature) was relaxed towards ERA5 in the tropical band 10S-10N. All fields shown are integrated over the layer 300-100 hPa. The upper panel shows the mean error at day 2 in the reference reforecast, with streamfunction (contoured), divergent wind (vectors) and the forcing of vorticity by the divergent winds (the 'Rossby Wave Source', shaded). The lower panel shows the difference (relaxation minus reference reforecast) at day 2. Black contours and vectors, and the more saturated colours in the colour bar key, indicate statistical significance at the 5% level.

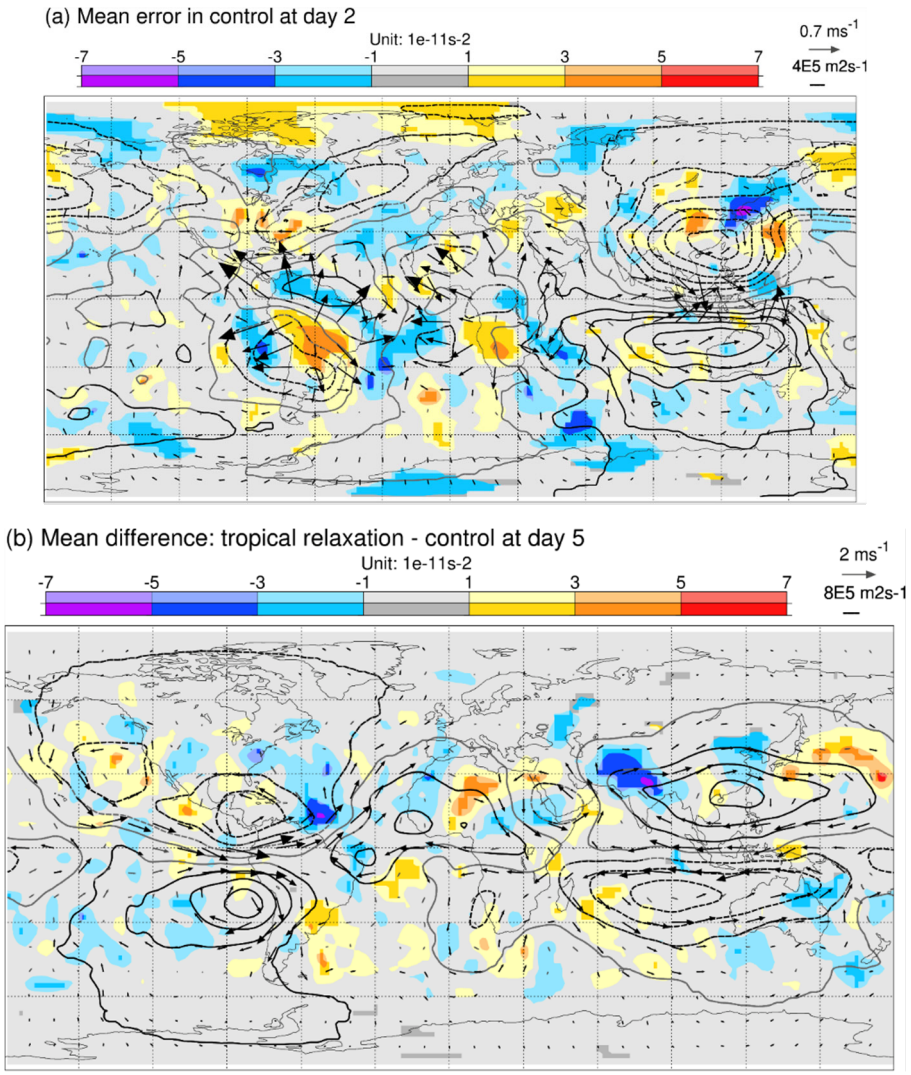

Figure 13: Plots based on the control (unperturbed) reforecasts covering the period DJF 2000-2016 and equivalent reforecast experiments where the circulation (vorticity, divergence and temperature) was relaxed towards ERA5 in the tropical band 10S-10N. All fields shown are integrated over the layer 300-100 hPa. The upper panel shows the mean error at day 2 in the reference reforecast, with streamfunction (contoured), divergent wind (vectors) and the imbalance between the forcing of vorticity by the divergent and rotational winds (the sum of the 'Rossby Wave Source' and the advection of absolute vorticity by the rotational flow, shaded). The lower panel shows the difference (relaxation minus reference reforecast) at day 5, with streamfunction (contoured), rotational wind (vectors) and the advection of absolute vorticity by the rotational wind (shading). Black contours and vectors, and the more saturated colours in the colour bar key, indicate statistical significance at the 5% level.

Shading in Figure 13(a) shows the sum of errors in the mean Rossby Wave Source and errors in the advection of absolute vorticity by the rotational flow. This sum is non-zero around the jet entrance near Japan - indicating (in the barotropic vorticity equation) that the bias in the control reforecasts is evolving with lead-time, which is consistent with the changes noted above. Figure 13(b) shows the day 5 impact of the relaxation on the streamfunction (contours) and rotational winds (vectors). By day 5, the response has evolved somewhat from the direct Rossby wave signal and is beginning to extend over the Pacific,

where it strengthens the subtropical jet by around 1ms^{-1}. At longer lead-times, further interactions may mean that this response to tropical convection bias could complicate the identification of other factors influencing the subsequent weakening of the subtropical jet.

6.2 Other sensitivity experiments

In addition to the tropical relaxation experiment, a series of nudging experiments (Table 1) has been performed where other areas were nudged towards ERA5. Nudged areas include:

- Stratosphere
- Tibetan Plateau
- Mongolian Plateau
- Tibetan + Mongolian Plateau
- High latitude (North of 60N)
- Polar region (North of 70N)

Two additional sensitivity experiments were performed with:

- The turbulent orographic form drag (TOFD) reduced by 2/3
- Short tails for the turbulent mixing in the boundary layer.

Table 1: Description of the sensitivity experiments

Experiment ID	Description
hiws	47r1 – Reference
hl0v	Tropical relaxation
hk4j	Stratosphere relaxation
hjch	Tibetan Plateau relaxation
hk50	Tibetan + Mongolian Plateau
hl7w	Mongolian Plateau relaxation
hlot	Polar relaxation (>70N)
hm1h	High latitude relaxation (>80N)
hmge	High latitude for T and troposphere only
hm8e	Weak tropical relaxation (only T and Vorticity, only troposphere)
hmgo	47R3

The impact of all these experiments on the Pacific subtropical jet bias is summarized in Figure 14. This figure shows, for each experiment, the position of the jet (defined here as the eastward extension of the intensity of below 40 m/s) location where maximum U300 drops Pacific sub- and the intensity of the tropical jet.

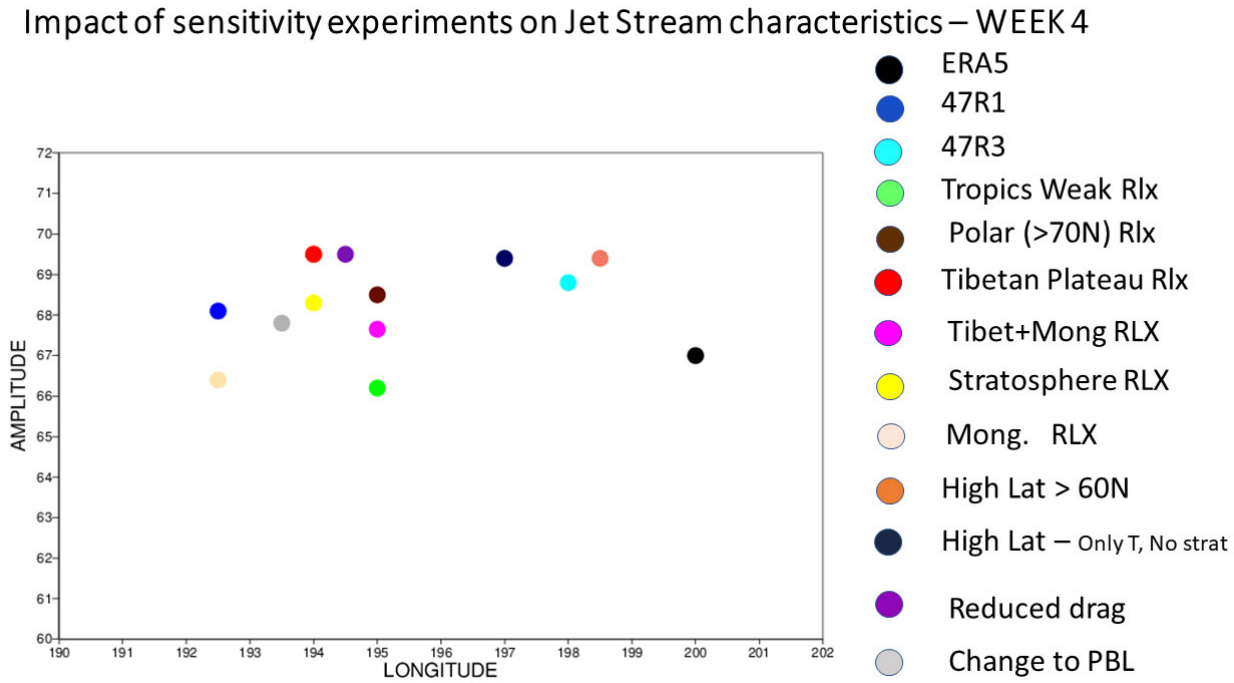

Figure 14: Pacific sub-tropical jet eastward extension (x-axis) and maximum amplitude (y-axis) in January in ERA 5 (black Circle) and at week 4 in the reference re-forecast experiment (Cycle 47r1, dark blue circle) and in several sensitivity experiments. The re-forecasts start twice a week over the period 2000-2018 with week 4 re-forecasts verifying in January.

Figure 14 confirms that the reference experiment at week 4 displays a Pacific sub-tropical jet located significantly more to the west (by about 8 degrees in cycle 47R1). As discussed above, relaxing the Tropics reduces slightly the westward shift by about 3 degrees and also the amplitude of the jet by about 2 m/s, which is more consistent with ERA5. Relaxing the stratosphere, the Tibetan Plateau or the Mongolian Plateau also leads to slight improvements, but not stronger than the tropical relaxation. Relaxing the Polar region (North of 70N) also reduces the westward extension bias by about 3 degrees, as with the tropical relaxation, but the amplitude of the jet is slightly increased. Finally, relaxing high latitudes (North of 60N) leads to the strongest reduction of the bias, with a difference of less than 2 degrees longitude from ERA5. This result suggests that model systematic errors between 60N and 70N are likely to play a role in the representation of the Pacific sub-tropical jet. This experiment was repeated, but this time only the troposphere and only temperature (instead of temperature, divergence and vorticity) were relaxed. In this experiment, the impact on the bias is not as strong as when relaxing temperature and winds in the troposphere and stratosphere, but it is still stronger than in all the other relaxation experiments. This confirms that the high latitudes play a particularly important role in the representation of the jet stream in the extended-range forecasts.

In order to assess the impact of the turbulent orographic drag and turbulent mixing parametrizations, which both affect surface drag, on the characteristics of the Pacific sub-tropical jet, two sensitivity

experiments were performed: the strength of the turbulent orographic form drag (TOFD) was reduced by 2/3, and short tails instead of long tails were used for turbulent mixing in the planetary boundary layer (see Sandu et al, 2013 for more details). Both changes led to a slight reduction of the bias, particularly the 2/3 reduction of TOFD which increased the amplitude of the jet and moved the eastward extension by about 3 degrees longitude to the east, which is closer to ERA5 (Fig. 14). The impact of the change to the turbulent mixing in planetary boundary layer is much smaller.

The impact of a change of gravity wave drag scheme was also tested for seasonal re-forecasts starting on 1st November 1998-2016 and verifying in January. These seasonal experiments, produced with Cycle 46r1 and forced by observed sea surface temperatures, were performed in order to evaluate the effect of improvements to the orographic drag scheme planned to be introduced in cycle 48r1 (experiment hevr). These changes give an overall increase in orographic drag in the northern hemisphere winter. As shown in Figure 15, this has a beneficial impact on the 200 hPa zonal winds biases in the Pacific basin, reducing the westward bias in the subtropical jet, which has a similar pattern as in the extended range.

Finally, a set of extended-range re-forecasts has been produced with cycle 47r3 (cyan circle in Figure 14). According to Figure 14, there has been a clear improvement between cycle 47r1 and 47R3 in the representation of the Pacific jet stream. The bias has been significantly reduced by about 2/3 and the impact of 47r3 is close to the impact of relaxing the high latitudes. The strength of the Pacific sub-tropical jet (measured as the maximum value of U300 over the area 90E-140W, 20N-40N) is slightly higher than in 47R1. This improvement cannot be attributed to the difference of vertical resolution between 47r1 and 47r3 in operations (91 vs 137 vertical levels) since all the experiments were run at the same horizontal and vertical resolution (137 vertical levels). The improvement in the 47R3 experiment is likely due to the changes to the moist physics introduced in 47r3 which led to a stronger MJO and an increased wave activity in the IFS.

As mentioned in the introduction, the main motivation for this study was to improve the representation of MJO teleconnections, which may be affected by biases in the Pacific sub-tropical jet. Therefore, the sensitivity experiments which improved the representation of the Pacific subtropical jet stream should display more realistic MJO teleconnections. Figure 16 shows the composite of 500 hPa geopotential height 3 pentads after an active MJO over the Indian Ocean (MJO Phases 2 and 3). Although none of the model integrations produce MJO teleconnections over the Euro-Atlantic sector as intense as ERA5, the Tropics and Tibetan Plateau relaxation experiments, as well as the experiment with a change to the turbulent orographic drag coefficient, display more realistic teleconnections over the Euro-Atlantic sector. These experiments had a smaller bias in the Pacific jet stream than the reference experiment. However, 47r3, which displayed only a small bias in the eastward extension of the Pacific jet stream, does not produce significantly more realistic MJO teleconnections over the North Atlantic, suggesting that fixing the sub-tropical jet bias is not enough to improve the MJO teleconnections. Other model errors, such as the model deficiencies in the stratospheric pathway of the MJO teleconnections, may play a predominant role. The high latitude relaxation experiments have not been included in this analysis since the MJO teleconnection area in the North Atlantic is partially included in the relaxation area.

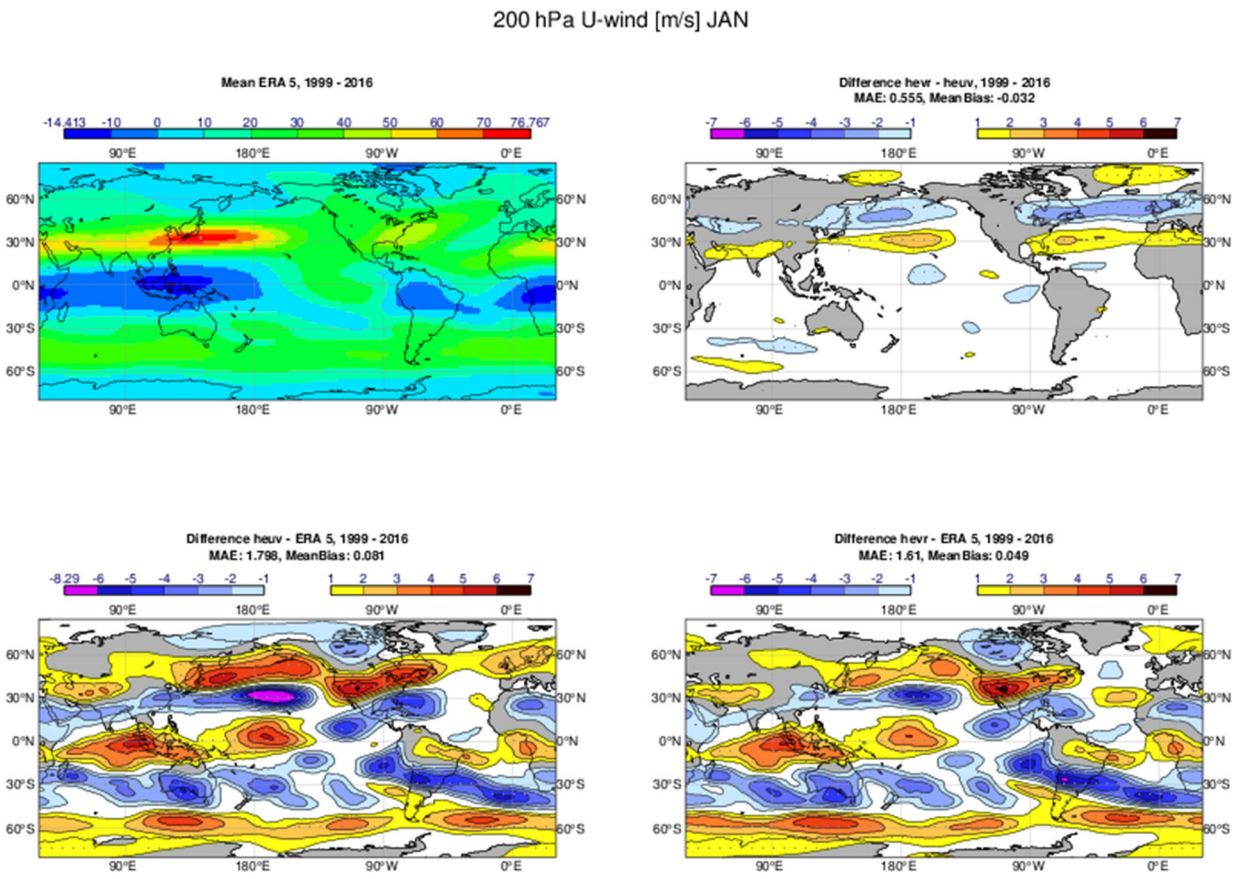

Figure 15: Climatological 200 hPa zonal winds in ERA5 (top left panel) for January 1998-2016. The bottom panels show the biases (relative to ERA5) in 200 hPa zonal winds in the control 46r1 re-forecast experiment (bottom left panel) and the re-forecast experiments using the revised gravity wave drag scheme proposed for cycle 48r1 (bottom right panel). The top right panel shows the difference between the two experiments. The re-forecasts start on 1st November and verify in January of 1998 through 2016 and have ten ensemble members."

An NAO index has been defined by projecting the composites of 500 hPa geopotential height onto an EOF which has been computed from NCEP re-analysis. According to Figure 17, the NAO indices associated with the composites displayed in Figure 16 tend to be slightly higher in the sensitivity experiments than in the reference experiment, but still far from ERA5, indicating just a slight improvement in the modulation of the NAO by the MJO, despite significant reductions of the Pacific jet stream bias.

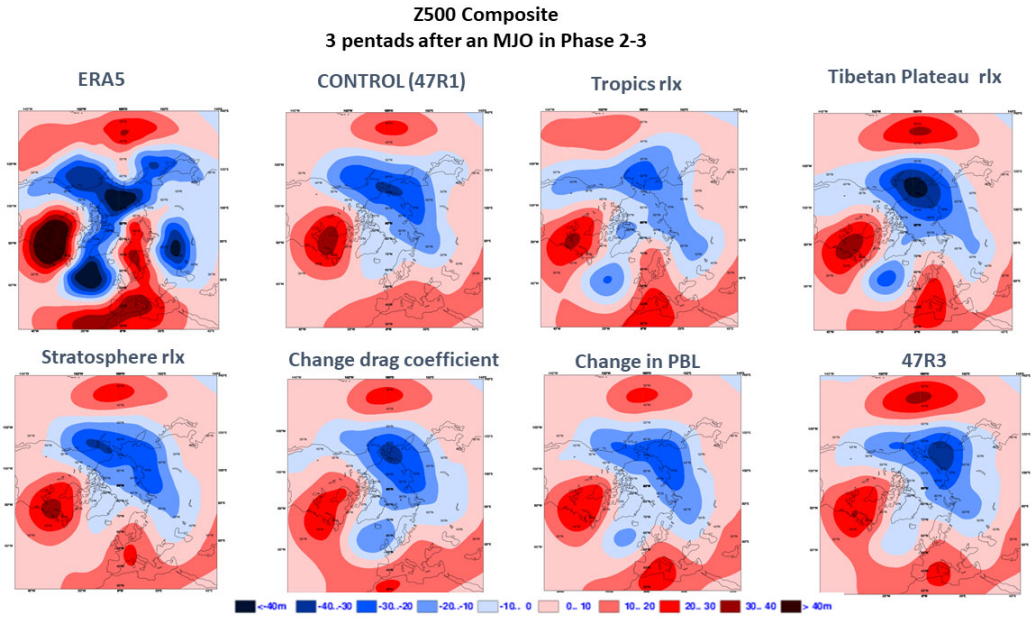

Figure 16: Composite of 500 hPa geopotential height anomalies 3 pentads after an MJO in Phase 2 or 3 in ERA 5 (top left panel), 47r1 (top, second left), and several relaxation and sensitivity experiments.

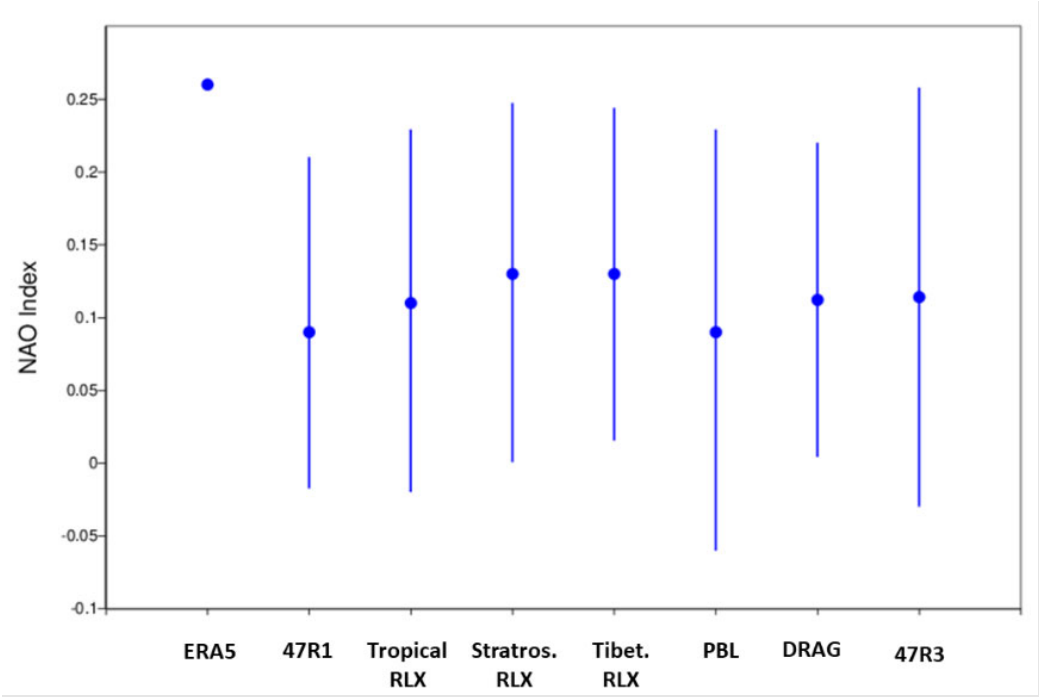

Figure 17: Amplitude of the NAO index from the composites in Figure 15. The vertical bars represent 2 standard deviations.

7. Conclusion and future directions

This study has shown that the Pacific sub-tropical jet eastern extension moves westward with lead time in the extended-range forecasts (weeks 1 to 4). This issue can be diagnosed as a negative bias in the 300 hPa zonal wind over the central North Pacific. It is present in most S2S models, except the NCEP model CFS2. This bias in the extended-range forecasts seems to be linked to errors at day 1 over Sea of Japan. A series of sensitivity experiments where part of the atmospheric circulation is nudged towards ERA5 suggests that there is not a unique source for this bias. However, model errors in the high latitudes seem to be a major contributor. Errors in the Tropics also have an impact, although not as strong. The bias has been considerably reduced in cycle 47R3, thanks to the changes to the moist physics. Despite this strong reduction, the representation of the impact of the MJO on the NAO has been only moderately improved. The difference in the bias between the control and perturbed members (whereby the control forecast exhibited a much stronger bias in 46r1 and 47r1) has also been significantly reduced in cycles 47r2 and 47r3.

There are plans to continue monitoring this bias in future model development. This would involve producing plots similar to figures 1, 4, 6, 9, 10 and 12(a) for each new model cycle. Future studies will also investigate the modulation of the Pacific jet by ENSO and decadal variability.

References

Jiang, X. et al., 2020: Fifty years of research on the Madden-Julian Oscillation: Recent progress, challenges, and perspectives. JGR Atmospheres, 125 (17), e2019JD030911, https://doi.org/10.1029/2019JD030911

Lee, Y.-Y. and Lim, G.-H., 2012: Dependency of the North Pacific winter storm tracks on the zonal distribution of MJO convection, JGR Atmospheres, 117, D14101, https://doi.org/10.1029/2011JD016417

Lee, R. W., Woolnough, S.J., Charlton-Perez, A.J. & Vitart, F., 2019: ENSO modulation of MJO teleconnections to the North Atlantic and Europe. Geophysical Research Letters, 46, 13535– 13545. https://doi.org/10.1029/2019GL084683

Sandu, I., Beljaars, A., Bechtold, P., Mauritsen, T. and Balsamo, G.: Why is it so difficult to represent stably stratified conditions in numerical weather prediction (NWP) models? *J. Adv. Model. Earth Syst.*, 5, 117– 133, doi:10.1002/jame.20013.

Vitart, F., 2017: Madden—Julian Oscillation prediction and teleconnections in the S2S database. Q.J.R. Meteorol. Soc, 143: 2210-2220. https://doi.org/10.1002/qj.3079

Vitart, F. and co-authors, 2019: Extended-range prediction. ECMWF Technical Memorandum, 854, 58 pp.

Zhou, W., Yang, D., Xie, SP. et al., 2020: Amplified Madden–Julian oscillation impacts in the Pacific–North America region. Nat. Clim. Chang. 10, 654–660. https://doi.org/10.1038/s41558-020-0814-